

Received October 20, 2019, accepted November 5, 2019, date of publication November 14, 2019, date of current version November 27, 2019.

Digital Object Identifier 10.1109/ACCESS.2019.2953546

A Biomimetic Flexible Fishtail Embedded With Shape Memory Alloy Wires

JIAN LI¹, (Member, IEEE), JUNMIN HE¹, YANGWEI WANG¹, (Member, IEEE),
KAI YU², MARCIN WOŹNIAK³, AND WEI WEI⁴

¹College of Mechanical and Electrical Engineering, Northeast Forestry University, Harbin 150040, China

²College of Mechanical and Electrical Engineering, Nanjing University of Aeronautics and Astronautics, Nanjing 210016, China

³Institute of Mathematics, Silesian University of Technology, 44-100 Gliwice, Poland

⁴College of Computer Science and Engineering, Xi'an University of Technology, Xi'an 710048, China

Corresponding authors: Yangwei Wang (wywkly@126.com) and Wei Wei (taneo@126.com)

This work was supported in part by the Fundamental Research Funds for the Central Universities under Grant 2572018BF04, in part by the National Natural Science Foundation of China under Grant 51905084, in part by the National Key Research and Development Program of China under Grant 2018YFB0203901, and in part by the Key Research and Development Program of Shaanxi Province under Grant 2018ZDXM-GY-036.

ABSTRACT In this paper, a biomimetic flexible fishtail actuated by shape memory alloy (SMA) wires is presented. The detailed structure of the fishtail propeller is designed to mimic the muscle and bone structure of a *Carassius auratus*. The mechanical modeling of the biomimetic fishtail is built; then, constitutive equations and thermal models of embedded SMA wires are described. Next, experiments are carried out to analyze the propulsive performance of the fishtail. Its maximum bending angle is 50° under the conditions of a heating voltage of 14.8 V and a heating time of 175 ms at a water temperature of 24.5°C. The symmetrical characteristic of both sides of the biomimetic fishtail is good, and different fluctuation can be adjusted by changing the heating time. The bending time and recovery time are recorded, and the effect of heating time on oscillation frequency is analyzed. Finally, the propulsive forces of three different heating modes at frequencies of 0.4 Hz, 0.5 Hz and 0.6 Hz are tested and compared. A relatively good heating mode is discovered for controlling the biomimetic fishtail during the experiments. The biomimetic fishtail obtains the largest average propulsive force of 0.041 N at a frequency of 0.8 Hz with a heating time of 80 ms and a bending angle of 22°.


INDEX TERMS *Carassius auratus*, biomimetic fishtail, SMA wire, flexible oscillation, propulsive performance.

I. INTRODUCTION

Similar to forests [1], the ocean is also an important resource for humans. It is very important to explore and monitor oceans. Underwater robots have played increasingly important roles in exploring oceans. For example, a robotic fish developed by Katzschmann R.K was used to explore underwater life [2], [3]. Generally, traditional underwater robots are propelled by screws driven by motors. While they have the advantage of many functions, they also have obvious defects: low efficiency, low mobility, miniaturization difficulty, high noise, and poor bio-friendliness [4]. Aquatic animals such as fish have experienced billions of years of natural selection and have evolved a superb swimming ability to achieve high

speed and efficiency [5]. Inspired by these, in response to the problems of traditional underwater robots, researchers have developed a variety of bionic underwater robots to meet different needs, such as robotic fish [6], robotic lobsters [7], robotic turtles [8] and robotic jellyfish [9]–[12].

Most bionic underwater robots are still driven by motors, which have the disadvantages of a complex structure and high noise. Their swimming performance is still far behind that of underwater creatures [13]. For this reason, in the past decade, more research has focused on the application of intelligent material-driven artificial muscles to bionic underwater robots [14]. Robotic fish driven by smart materials such as SMA (shape memory alloy) [15], [16], IPMC (ion-exchange polymer metal composite) [17], [18], piezoceramics [19], [20], polypyrrole [21] and fluid [22] were developed. Bionic robotic fish have become highly flexible,

The associate editor coordinating the review of this manuscript and approving it for publication was Derek Abbott .

simple in structure and small. These factors also effectively improve their propulsion performance.

Fish are the most common aquatic organisms, and their propulsion modes are divided into BCF (body and/or caudal fin) and MPF (median and/or paired fin) modes [23]. Correspondingly, bionic robotic fish are also divided into BCF [24] and MPF modes [25]. The BCF mode is faster, but the MPF mode is more maneuverable. Among the smart materials, SMA has the disadvantages of slow cooling and high power consumption, but its ability to withstand strain and stress is relatively great, and its performance approximates that of muscle fibers. Therefore, SMAs are widely used in robots [26]. Using SMAs, researchers have developed a lot of robotic fish and bionic propellers [27]–[30], which have achieved good biomimetic performance.

However, most of the bionic fish mentioned in previous research achieved their flexibility by means of several joints or a thin sheet-shaped tail. The structure of the bionic fish which use several joints is complicated. The shape of the tail which use a thin sheet is difficult to fit to the head compartment to form a streamlined whole. Its structural characteristics and driving means also make it difficult to develop a bionic fishtail that has high similarity to an actual fishtail. This research aims to develop an SMA-driven bionic fishtail combined with the muscle arrangement of fish swimming in the BCF mode. It has a real fishtail shape and can achieve flexible movement with large amplitude. The morphology of the *Carassius auratus* and the structure of the biomimetic fishtail are introduced in Section II. Mechanical modeling of the biomimetic fishtail is carried out to obtain the relation formula of the stress and strain of SMA wires with different bending angles in Section III. Section IV introduces the constitutive model of SMA and the thermodynamical equilibrium equation of SMA. The experimental results and effects of the actuation properties on the oscillation of the fishtail and force generation are discussed in Section V. Section VI concludes the work and makes some recommendations for future research.

II. DESIGN OF THE BIOMIMETIC FISHTAIL

A. BIOLOGICAL FOUNDATIONS AND CHARACTERISTICS OF A FISHTAIL

According to fish swimming modes, the biomimetic underwater robots are divided into body/tail fin (BCF) swimming mode and the central fin/fin (MPF) swimming mode [31]. Most fish in nature employ the BCF swimming mode. Compared with the other mode, the BCF mode provides higher swimming speed and higher swimming efficiency. The BCF swimming mode can be mainly subdivided into anguilliform, carangiform, and thunniform modes, as shown in Fig. 1.

The anguilliform mode involves the whole body in undulation, the carangiform mode restricts undulation to the rear half of the body, and the thunniform mode uses only the rear third of the body [23]. The carangiform mode has the best balance between speed, acceleration and controllability [32]. Thus, we employed this mode to develop a biomimetic robotic fish.

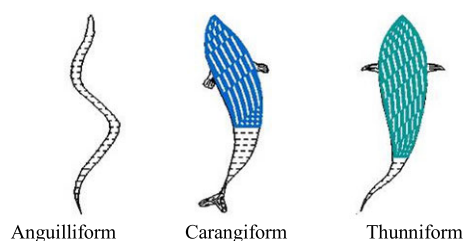


FIGURE 1. Three main kinds of BCF modes.

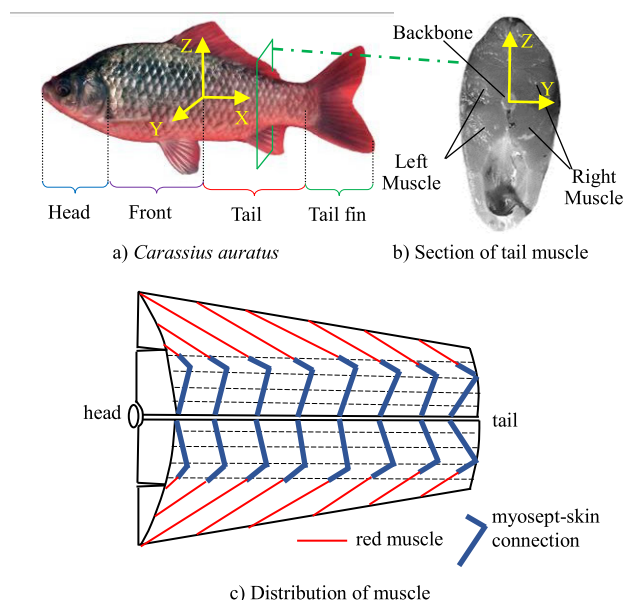


FIGURE 2. Biomimetic prototype.

Carassius auratus (see Fig. 2a), which is a kind of typical carangiform fish, generates thrust by bending its fishtail. As shown in Fig. 2b and Fig. 2c, the muscles are distributed on the left and right sides of the fish’s backbone, and on each side, the muscle fibers are mainly distributed up and down the sides of the backbone.

During steady swimming, *Carassius auratus* alternately contracts its muscles on the two sides of the backbone and relaxes the muscle on the opposite side to swing the tail and tail fin. The oscillation motion forms the anti-Karman vortex street, which induces a backward jet flow along the fish’s body. In addition, *Carassius auratus* can accordingly obtain a forward reacting force from the jet flow [33].

To establish 3D modeling of the biomimetic fishtail, a coordinate system is incorporated, as shown in Fig. 2 and Fig. 3. We define the backward direction along the fishtail as the x-axis positive direction, the horizontal direction to the left of the fish as the y-axis positive direction, and the vertical upward direction as the z-axis positive direction. The coordinate system is set in the center of the cross section of the fishtail. Then, the dimensions of the *Carassius auratus* sample’s cross sections are simplified as ellipses and measured; the maximum sizes in the X, Y and Z directions are 135 mm, 72 mm and 33 mm, respectively. With the 3D modeling

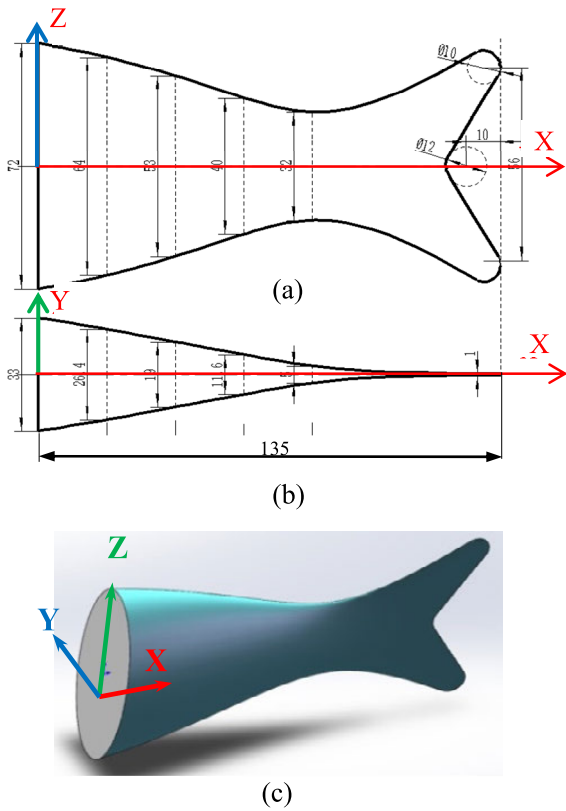


FIGURE 3. The appearance of the biomimetic fishtail.

software SolidWorks, we completed the appearance design of this robotic fishtail (see Fig. 3), which imitates the fishtail of the *Carassius auratus* sample, to ensure the appearance is streamlined.

B. MECHANICAL STRUCTURE

To imitate the distribution of muscle fibers and backbone in *Carassius auratus*, SMA wires are selected to mimic the function of those muscle fibers, and an elastic substrate is used to mimic the backbone of *Carassius auratus*. The arrangement of the SMA wire of the bionic fishtail in this paper mimics the muscle arrangement of the fish body [34]. Two SMA wires of different lengths positioned on either side of the fishtail are driven in stages, making it possible to simulate both undulation and pure oscillation. To achieve a large bending angle, the bionic structure is designed with the SMA wires attached to the surface of the elastic substrate (see Fig. 4).

The SMA wires are divided into two groups: SMA_A (SMA_A1 and SMA_A2) and SMA_B (SMA_B1 and SMA_B2). SMA_A1 and SMA_B1 are longer than SMA_A2 and SMA_B2. Actuating any one group results in a flexible bending of the bionic structure. The maximum bending angle can be attained by actuating SMA_A1 or SMA_B1.

Fig. 5 shows the detailed design of the biomimetic fishtail. Each bundle of the SMA wires is arranged in the shape of a trapezoid, and 0.2-mm-diameter SMA wires

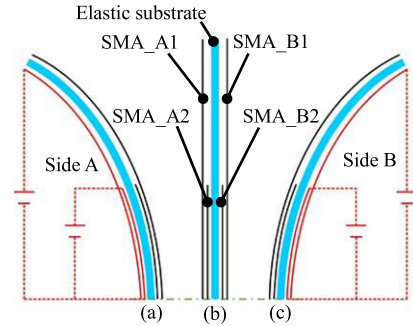


FIGURE 4. Schematic diagram of the actuation structure. (a) Bending to side A. (b) Initial position. (c) Bending to side B.

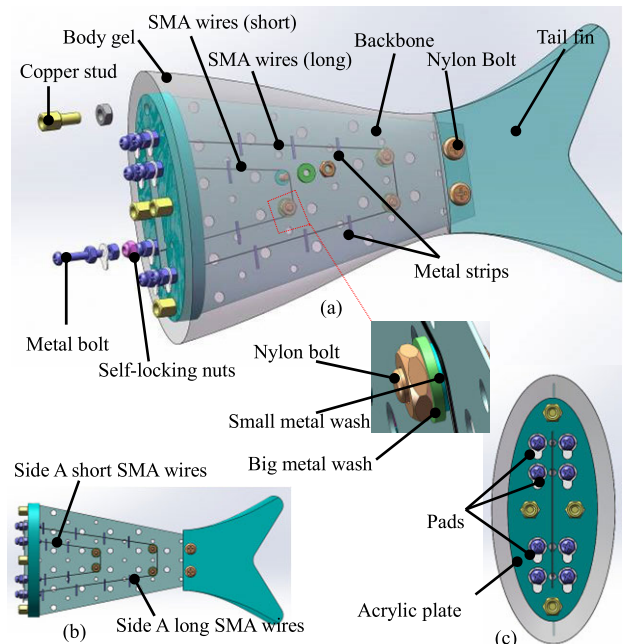


FIGURE 5. The structure of the biomimetic fishtail. (a) exploded views. (b) SMA wires distribution view without body gel. (c) joint structure.

(Ni–Ti, produced by Grikin Advanced Materials Co., Ltd., China) are employed. A glass fiber sheet with a thickness of 0.3 mm is chosen as the backbone of the robotic fishtail, and its characteristics of resistance to high temperatures, high hardness, good insulation and good elasticity give it superior performance as the backbone of the biomimetic fishtail. The backbone is designed to be fixed in an acrylic plate. Four copper studs are fixed in the acrylic plate for connecting the biomimetic fishtail to the front of the robotic fish. Both ends of the SMA wires are fixed in the acrylic plate by a screw bolt with self-locking nuts and pads. The nuts are used to maintain tension in the SMA wires, and the pads are used to weld current leads.

To prevent the silicone gel from breaking off due to the large stress that occurs when the SMA contracts [35], [36], metal aluminum strips, with a size of $0.2 \times 0.6 \times 6$ mm, are fixed on the glass fiber sheet. Another function of the metal aluminum strips is to help dissipate heat from the SMA wires

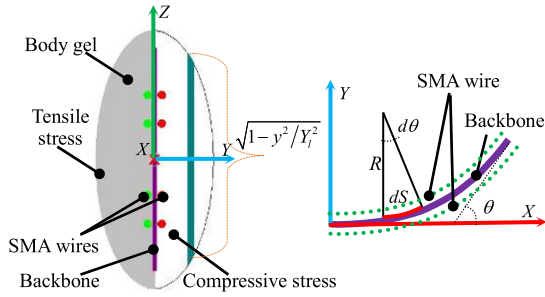


FIGURE 6. Microstructure of a bent biomimetic fishtail.

heat. The tail fin is made of 0.3-mm-thick polyvinyl chloride (PVC). We designed the bionic fishtail to be streamlined using EON-01 silicone gel (produced by Shenzhen Yi Xing Chemical Co., Ltd., China) as the infilling and skin to shape the fishtail. Therefore, the fishtail is flexible and insulated, and its flexibility approximates that of real muscle. The glass fiber sheet and silicone gel can not only store elastic energy when the fishtail bends but can also release elastic energy when the fishtail recovers. In this way, the energy use ratio is higher because of the elastomer [22].

III. THEORETICAL ANALYSIS OF THE BIOMIMETIC FISHTAIL

A. MECHANICAL MODELING

Based on the measured parameters, the edge profilogram of the biomimetic fishtail is simplified and fitted to two linear functions in the first quadrant of the coordinate system by MATLAB. The coordinate function of points on the contour curve in the Y direction and the Z direction, Y_l and Z_l , is

$$\begin{cases} Y_l = -0.177x + 0.0166 \\ Z_l = -0.26x + 0.0365, \end{cases} \quad 0 < x < l \quad (1)$$

where l is the length of the biomimetic tail segment.

When the SMA wires embedded in the biomimetic fishtail are heated, their contraction forces the fishtail to bend. A cross section unit of the biomimetic fishtail is chosen (see Fig. 6). When the biomimetic fishtail bends to a facilitative angle, the moment produced by the SMA wires, silicone gel and glass fiber sheet achieves a balance in the section. In the figure, S is the distance of the curved unit along the curve to the origin. The resultant moment function is given by

$$M_f + M_b + M_g = 0 \quad (2)$$

where M_f is the moment produced by SMA wires, and M_b and M_g are the resistance moments of the silicone gel and glass fiber sheet, respectively.

The moment of n SMA wires is calculated, as follows

$$M_f = 2n\pi hr^2(\sigma - \sigma_0) \quad (3)$$

where σ is the heating stress of SMA wires; σ_0 is the initial stress of the SMA wires; h is the distance from

TABLE 1. The mechanical parameters of the bionic structure.

parameters	values
l	6×10^{-2} m
n	$n=2$ ($0 < x \leq l/2$) $n=1$ ($l/2 < x \leq l$)
σ_0	100 MPa
h	4.5×10^{-4} m
r	1×10^{-4} m
E_s	4 MPa
k_g	$(0.26x + 0.087) \times 10^{-3}$ N m / °

an SMA's center of a circle to a neutral surface; and r is the radius of the SMA wires.

The moments of the silicone gel and glass fiber sheet are calculated as follows

$$\begin{aligned} M_b &= \int_{-Y_l}^{Y_l} E_S \kappa y b dy = \int_{-Y_l}^{Y_l} E_S \kappa y \sqrt{1 - \frac{y^2}{Y_l^2}} dy \\ &= \int_{-Y_l}^{Y_l} E_S \frac{1}{l/\theta} y \sqrt{1 - \frac{y^2}{Y_l^2}} dy \end{aligned} \quad (4)$$

$$M_g = k_g \theta \quad (5)$$

where E_S is the Young's modulus of the silicone gel; κ is the curvature, and the value is $1/R$. R is the radius of curvature, and the value is l/θ . θ is the bending angle of the section; k_g is rotational stiffness of glass fiber sheet based on experimental data fitting.

The strain ε of the SMA wires at θ is

$$\varepsilon = \frac{h}{l} \theta \quad (6)$$

From equations (1) to (6), the relationship between the stress of SMA wire and the bending angle of the biomimetic fishtail can be obtained, and the mechanical parameters are shown in Table 1.

B. CONSTITUTIVE EQUATION OF SMA

SMA wires can produce a large deformation under small stress at low temperature; when its temperature rises up to a certain value, it will return to the original shape, and this characteristic is known as the shape memory effect (SME) [37], as shown in Fig. 7.

At low temperatures, when plastic prolongation happens to SMA wire due to the action of a force, its internally twinned martensite phase becomes stress-induced martensite, and its length increases. After its temperature rises to the phase transition temperature, the microstructure changes from martensite to austenite, and its length returns to the initial length. After the SMA wires cool to a low temperature, the internal austenite phase changes to a twin martensite phase, and the length remains unchanged.

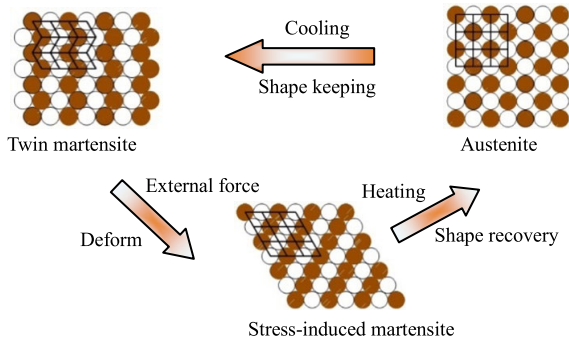


FIGURE 7. Schematic of the SMA phase transition.

To obtain the relation between temperature, stress and strain of the embedded SMA wires, the constitutive equation [38] is given by

$$\dot{\sigma} = E\dot{\varepsilon} + \Theta\dot{T} + \Omega\dot{\xi} \quad (7)$$

$$\xi_A = \frac{1}{2}[\cos(a_A(T - A_s) + b_A\sigma) + 1] \quad (8)$$

where ξ is the phase transformation fraction; T is the temperature of the SMA wires; Θ is the thermal expansion factor; $\Omega = -\varepsilon_L E$ is the phase transformation coefficient; ε_L is the remanent strain; $E = E_A + \xi(E_M - E_A)$ is the Young's modulus of the SMA; E_A is the Young's modulus of the austenite; E_M is the Young's modulus of the martensite; ξ_A is the heating phase transformation fraction; A_f is the phase transformation final temperature; A_s is the austenite phase transformation start temperature; $a_A = \pi/(A_f - A_s)$ is the austenite amplitude factor; $b_A = -(a_A/C_A)$ is the stress coefficient; and C_A is the fitting parameter.

C. THERMAL MODEL OF THE SMA

In this work, electrical heating is applied to actuated SMA wires. Hence, the heat transfer equation for an SMA wire that includes electrical heating and natural convection is given by

$$mc_p \frac{dT}{dt} + h_c A_c (T - T_0) = \frac{V^2}{R} \quad (9)$$

where $m = \rho_m A l_{SMA}$ is the mass of the SMA wires; ρ_m is the density; A is the cross section area; l_{SMA} is the length of one SMA wire; c_p is the specific heat capacity of the SMA wires; T_0 is the ambient temperature; h_c is the heat convection coefficient; A_c is the surface area of the SMA wires; $R = \rho l_{SMA}/A$ is the resistance of the SMA wires; ρ is the resistivity of the SMA wires; t is the heating time; V is the heating voltage, and h_c is the heat dissipation coefficient of SMA wire.

All the parameters of the SMA wires are shown in Table 2.

IV. EXPERIMENTAL SETUP

To measure and analyze the flexible oscillatory motions of the biomimetic fishtail, five signal points, P1-P5, are marked on the top edge surface of the biomimetic fishtail (see Fig. 8). P5 is at the end of the long wires, and P3 is at the end of the short wires.

TABLE 2. Table II [38]. The actuated parameters.

parameters	Values
Θ	0.55 MPa/□
Ω	-1.12 Gpa
E_A	65 GPa
E_M	26.69 GPa
A_f	78 □
A_s	66 □
a_A	0.31 □ ⁻¹
C_A	13.8 × 10 ⁶
ρ_m	6.5 × 10 ⁻³ kg/m ³
c_p	870 J / (kg · °C)
T_0	24.5 □
ρ	1.11 × 10 ⁻⁶ Ω · m

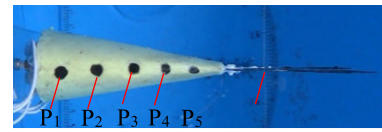


FIGURE 8. Points marked on the fishtail.

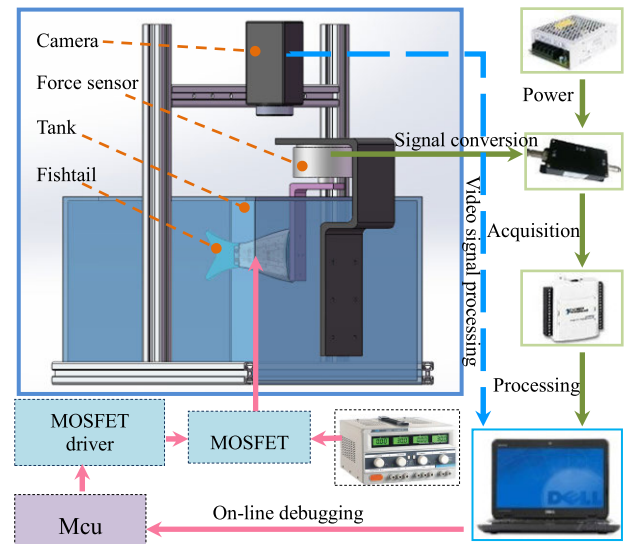


FIGURE 9. Experimental conditions and signal measurement system.

Fig. 9 shows the experiment system that consists of tank, camera, force sensor, microcontroller unit (MCU), adjustable power, data acquisition card and computer. All the actuating experiments are carried out in a tank with a length of 450 mm, width of 300 mm and depth of 250 mm. The images of the experiments are taken with an HD digital camera (HDR-CX610E made by Sony) at a speed of 25 frames per second. Hydrodynamic forces are detected by an LDCZL-MFT three-dimensional force sensor (produced by Beijing Longding

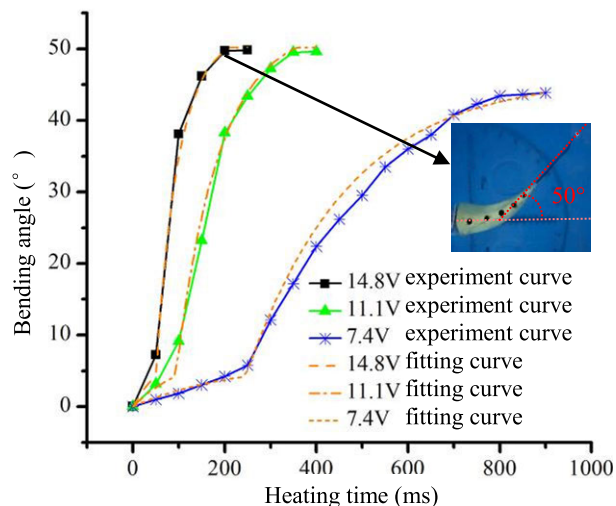


FIGURE 10. The relation between the bending angle and heating time actuated by different voltages.

Jinlu Control Technology Co., Ltd., China); its ranges are $F_x = F_y = \pm 10$ N, $F_z = \pm 20$ N. All the data are acquired with a signal acquisition card (NI-USB-6009). The heating current is supplied by an adjustable power (Qj-3003s) with a maximum voltage of 30 V and a maximum current of 6 A. The control circuit mainly consists of a MCU (microcontroller unit) (STC90C516), 4 MOSFET switches (IRF3808) and one MOSFET driver (L293D). The computer is responsible for information integration and processing.

V. RESULTS AND DISCUSSION

A. RELATION BETWEEN HEATING TIME AND BENDING ANGLE

We heat SMA_A1 and SMA_B1 to obtain the largest bending angle that the fishtail can realize at different heating times. The temperature of the water is 24.5°C. Actuating voltages of 7.4 V, 11.1 V and 14.8 V are selected. Considering that the resistance of the SMA wires is approximately 2 Ω, the input power is between 27 and 109 W. The initial heating time of each SMA wire is 50 ms, and it increases by 50 ms in each experimental group. The interval time between each heating operation is set at 60 s so that the SMA wire is cooled as much as possible. Fig. 10 shows the status of bending angles at different heating times. The bending angle increases with an increase in heating time, and a higher voltage can produce a faster bending speed. The maximum bending angle is approximately 43° at the voltage of 7.4 V, and it needs 800 ms to reach that amount. At voltages of 11.1 V and 14.8 V, we can acquire a maximum bending angle of 50°. At 11.1 V, the heating time is 300 ms, and it is 175 ms at 14.8 V. Therefore, the voltage value has little effect on the maximum bending angle. The theoretical results of the bending angle with different h_2 are fitted to the corresponding experimental results, and the obtained maximum error is 7.5%. To obtain a higher actuating frequency, 14.8 V is chosen in the next experiments.

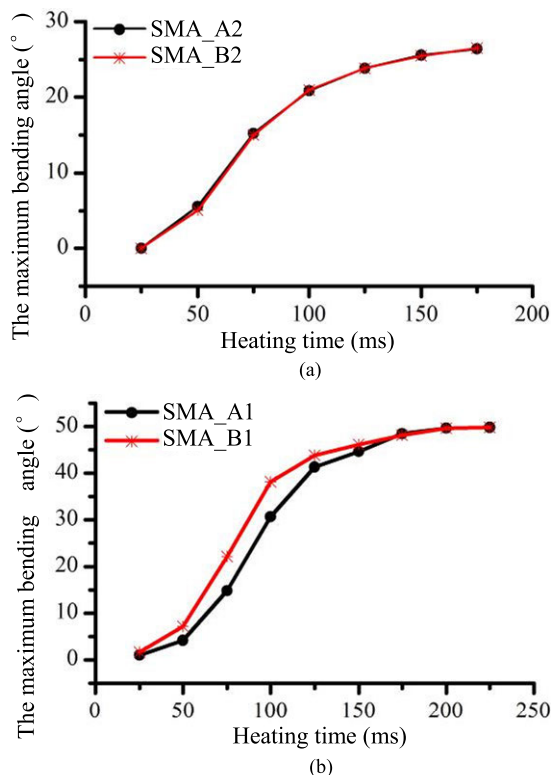


FIGURE 11. The relation between bending angles and heating times. (a) SMA_A2 and SMA_B2. (b) SMA_A1 and SMA_B1.

B. SYMMETRICAL CHARACTERISTICS OF BENDING MOTION

The swimming stability of the bionic robotic fish is mainly determined by the symmetrical characteristic when the biomimetic fishtail oscillates. Therefore, we tested the bending angles of the biomimetic fishtail on both sides with gradually increasing heating time; the initial heating time was 25 ms. The actuating rule is alternately heating SMA_A1 and SMA_B1 and SMA_A2 and SMA_B2 and recording the maximum oscillation angles on both sides. The relation between the maximum bending angles and heating times of the short SMA wires is shown in Fig. 11a. The pair of short SMA wires are found to have kept the ideal symmetrical characteristic. However, the long SMA wires are not similarly ideal; although their largest bending angles are alike, with the same bending angle, SMA_A1 needs more heating time (see Fig. 11b). The reason for this difference is that the tension of SMA_B1 is larger than that of SMA_A1, and the biomimetic fishtail bent to Side A generates more stress. Hence, the bending angle of Side B is higher than that of Side A at the incomplete phase transformation in the SMA wires. However, the maximum bending angle of both sides is the same at the complete phase transformation. In the next experiments, the heating time of SMA_A1 increases by 10 ms more than that of SMA_B1 for the oscillation balance of the biomimetic fishtail.

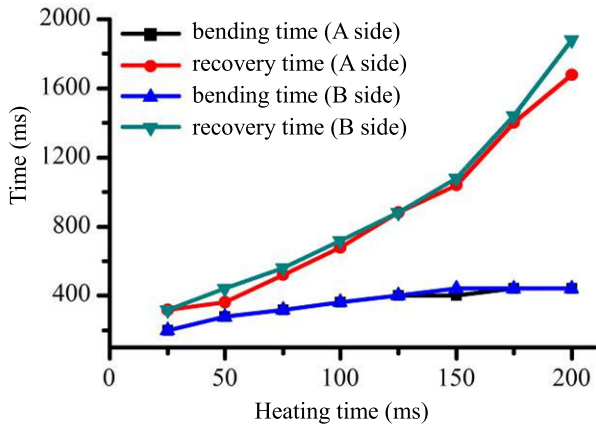


FIGURE 12. The bending time and recovery time at different heating times.

C. BENDING TIME AND RECOVERY TIME

In the process of oscillation, the biomimetic fishtail first oscillates from the initial position to the maximum angle position; the time this process takes is defined as the bending time. Then, the biomimetic fishtail oscillates from the maximum angle position to the initial position; the time this process takes is defined as the recovery time. The bending time and recovery time of the long SMA wires on both sides are tested. The bending time and the recovery time increase with an increased heating time (see in Fig. 12).

However, the bending time maintains a stable value of approximately 400 ms when the heating time is more than 125 ms. During the bending time, the stress of the SMA wires first increases and then decreases, and the force balance is achieved at the end of the bending time. The stress of heated SMA wires reaches its largest value when the heating process ends. Therefore, the heating time is shorter than the bending time, as is observed during the experiments.

As shown in Fig. 13, the larger the bending angle is, the longer the recovery time and bending time become. If the bending angle exceeds 40°, the recovery time will rapidly increase, but the bending angle will almost remain unchanged. When the bending angle is less than 40°, the recovery time is also much longer than the bending time. Therefore, the oscillation frequency of the biomimetic fishtail mainly depends on the value of the recovery time.

D. PROPULSIVE WAVE OF THE BIONIC FISHTAIL

When the flexible fishtail oscillates, we should heat all the long and the short SMA wires to take full advantage of their stress. There are three different modes in the heating sequence (see in Fig. 14): the first mode is to first heat the short SMA wires and then heat the long SMA wires; the second is to first heat the long SMA wires and then heat the short SMA wires; and the third mode is to alternately heat the long SMA wires and the short SMA wires by cyclic heating pulses, which has an equal pulse width and pulse interval of 10 ms. All the SMA wires are driven at a voltage of 14.8 V. In Fig. 14, T is the driving cycle of the entire bionic tail fin.

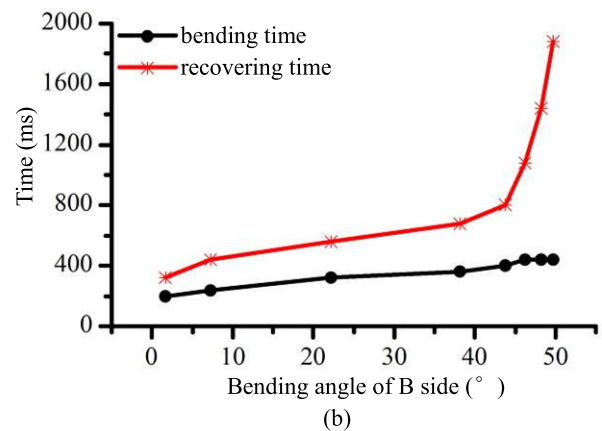
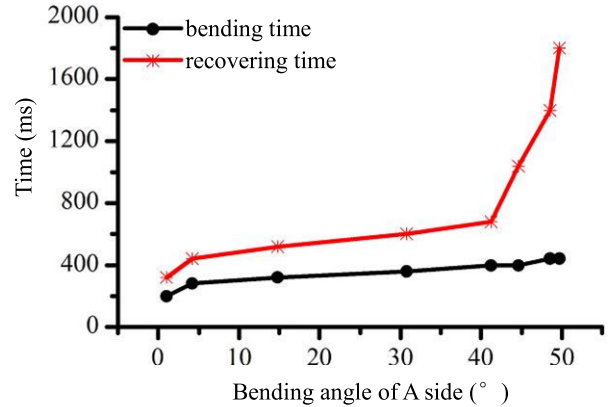


FIGURE 13. Bending time and recovery time at different bending angles.

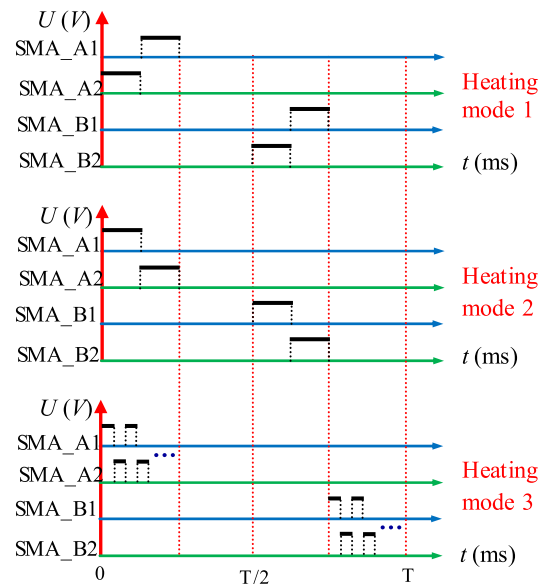


FIGURE 14. The heating pulse of the three heating modes.

The heating times of the three heating modes are identical. To determine which heating mode produces the best swimming performance, we compare the bending processes of three heating modes, and the long SMA wires and short SMA wires are heated for 120 ms each at

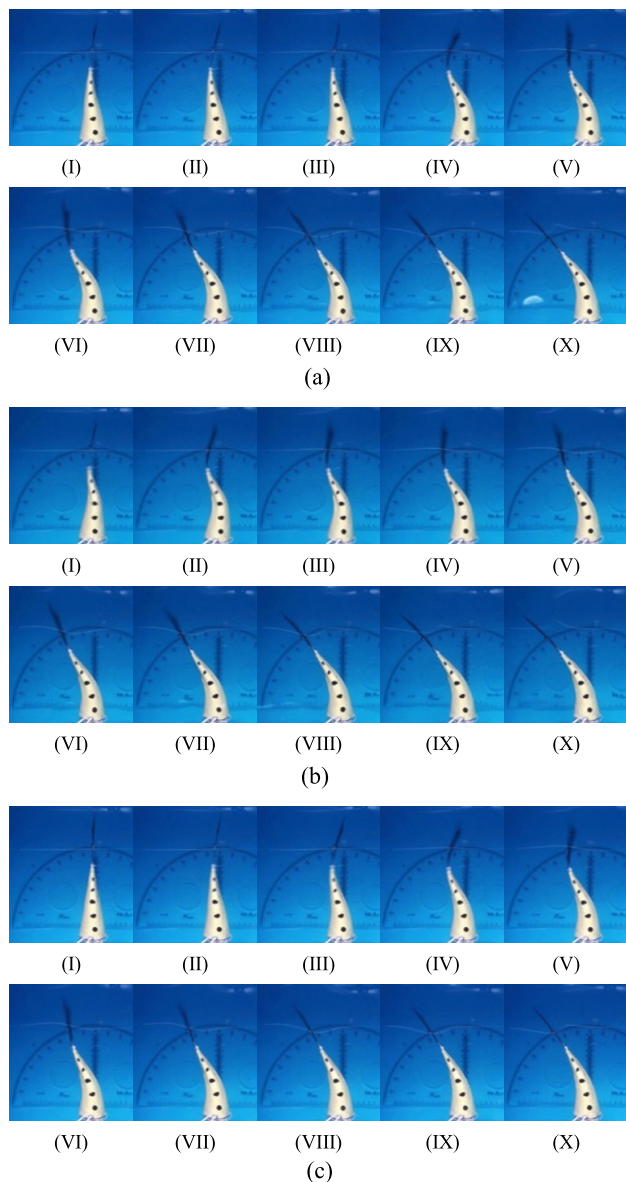


FIGURE 15. Bending process of three heating modes: (a) heating mode 1; (b) heating mode 2; (c) heating mode 3.

a 0.5 Hz oscillation frequency. The detailed bending process is presented in Fig. 15. The interval time between every image is 40 ms, and the whole process is 400 ms.

As seen from Fig. 15, the maximum bending angles of the three heating modes are close to each other (Fig. 15 (a) shows heating mode 1, Fig. 15 (b) shows heating mode 2, Fig. 15 (c) shows heating mode 3), but the bending processes differ. In heating mode 1 in Fig. 15 (a), images I-III show that the biomimetic fishtail is actuated by SMA_A2 and bends at P2 because SMA_A1 could actuate a larger bending angle than the short ones. When SMA_A1 shrinks in image IV, the biomimetic fishtail shows an obvious bending action at P3. In heating mode 2 in Fig. 15 (b), images I-III show that the biomimetic fishtail is actuated by SMA_A1 and bends at P4. Then, SMA_A2 shrinks in image IV, and the

TABLE 3. Propulsion in three heating modes and frequencies.

Heating mode	Frequency (Hz)	Average propulsion (N)	Peak propulsion (N)
Heating mode 1	0.4	0.017	0.123
	0.5	0.025	0.170
	0.6	0.033	0.242
Heating mode 2	0.4	0.014	0.202
	0.5	0.022	0.220
	0.6	0.030	0.221
Heating mode 3	0.4	0.017	0.137
	0.5	0.021	0.150
	0.6	0.028	0.142

bending point changes to P3. In heating mode 3 in Fig. 15 (c), SMA_A2 and SMA_A1 are heated alternately every 10 ms, and we consider that they are heated synchronously at the macro level. In this case, the bending point stays at P3 the entire time. The experiment results show that the biomimetic fishtail oscillates with good flexibility. The oscillating movement of the biomimetic tail segment was transmitted from the front part to the tail end in heating mode 1, and the movement was the opposite in heating mode 2, but the motion transmission was not obvious in heating mode 3. The tail fin of the bionic propeller could push water back with a great attack angle in heating mode 1 and heating mode 3, but the effect was not prominent in heating mode 2.

E. PROPULSIVE FORCE OF THE BIONIC FISHTAIL

To determine which heating mode has the best hydrodynamic performance, we test the propulsive force of the periodic oscillation process in three different modes. The propulsive forces were tested separately, showing two wave crests in each oscillation cycle of the biomimetic fishtail.

Fig. 16 shows the fluctuation process of the propulsive force at an oscillation frequency of 0.5 Hz and a heating time of 100 ms. In addition, 1 Hz is chosen as the low pass frequency filter of the propulsive force because of the symmetrical characteristic of both sides during oscillation. In heating mode 1, the average propulsive force is 0.025 N, and its peak value is 0.17 N. In heating mode 2, the average propulsive force is 0.022 N, and the peak value is 0.22 N. In heating mode 3, the peak value of the propulsive force is 0.15 N, and its average value is 0.021 N. By comparison, heating mode 1 has a gentler fluctuation of propulsive force, and its average propulsive force is the greatest. Hence, it is considered to be the best heating mode.

Oscillation frequencies of 0.4 Hz, 0.5 Hz and 0.6 Hz are used to test propulsive forces of three heating modes for further verification. Table 3 shows the average propulsive force

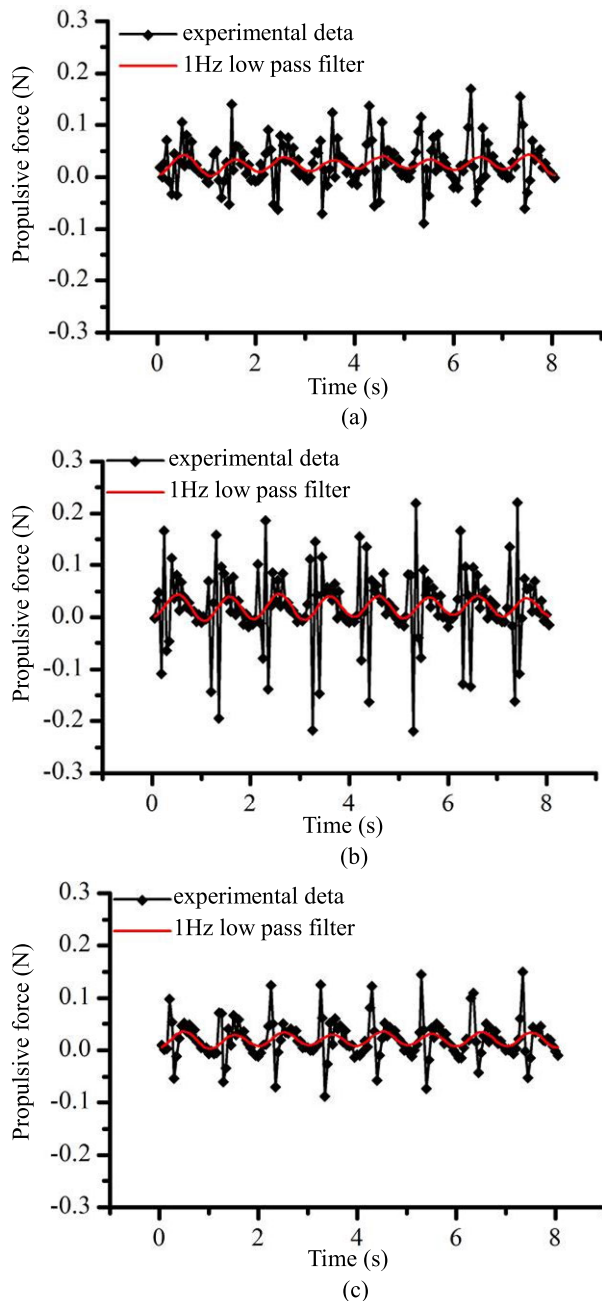


FIGURE 16. Propulsive force at a swinging frequency of 0.5 Hz. (a) heating mode 1. (b) heating mode 2. (c) heating mode 3.

and the peak propulsive force. They gradually increase with the increase in frequency. In addition, the average propulsive forces of heating mode 1 are maintained as the maximum in all three modes, and the peak propulsive forces of heating mode 3 are relatively small.

The higher oscillation frequency was attempted at a relatively small bending angle. At a heating time of 60 ms, the bending angle is 16° for the steady oscillating process. Fig. 17 shows the average propulsive force obviously grows larger with an increase of oscillation frequency until 1 Hz. After the swinging frequency goes beyond 1 Hz, the average

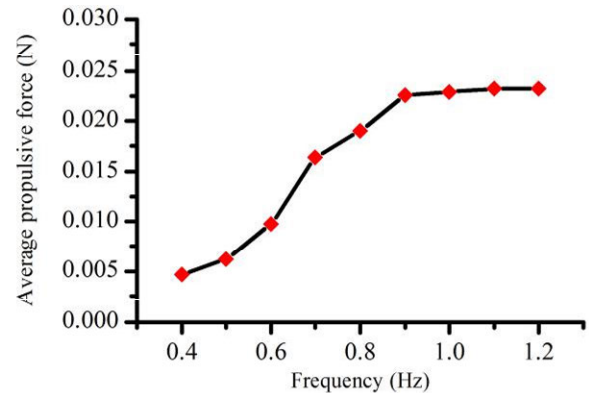


FIGURE 17. The average propulsive force with a heating time of 60 ms.

propulsive forces change very little. From the viewpoint of the energy utilization ratio, 1 Hz is better than higher oscillation frequencies with a heating time of 60 ms.

To investigate more possibilities, the oscillation frequencies from 0.4 Hz to 0.8 Hz are tested at heating times of 80 ms and a bending angle of 22° , and the largest average propulsive force produced at a frequency of 0.8 Hz is approximately 0.041 N. With a propulsive force condition at a larger bending angle of 37° and a heating time of 150 ms, the highest realizable oscillation frequency is 0.4 Hz, and the largest average propulsive force produced is approximately 0.022 N.

VI. CONCLUSION

In this paper, we introduce a biomimetic fishtail actuated by SMA wires that can flexibly oscillate by mimicking *Carasius auratus*. This work investigates a novel kind of bionic structure with good movement performance. The relationship between the heating times of the SMA wires and the bending angle of the biomimetic fishtail is obtained according to the mechanics mode, the constitutive equation and the thermodynamics mode. Experiments regarding the bending angle, oscillating symmetrical characteristic and different heating methods are carried out for further verification of the bionic capability. The results show that the bionic prototype can produce cyclic variations in propulsive forces with better oscillation flexibility. Multiple configurations of SMA wires of different lengths provide multiple driving strategies for bionic movement.

In fact, a 0.2 m-long fish has white muscle contractions as short as 0.02 s. Larger fish (0.7-1 m) have a steady tail beat of just over 1 Hz, and smaller fish (0.1-0.2 m) have a steady tail beat of 3-4 Hz [32]. The caudal fin of 30 cm fish produces 14 mN of thrust and 23 mN of lateral force, and the mean jet angle measured relative to the path of motion is 58° [39]. In comparison, in this paper, the minimum heating time of SMA wires is 0.05 s, and the maximum frequency is 1.2 Hz; the bionic fish tail can reach a maximum bending angle of 50° , and the average thrust force is approximately 21 mN. Comparing these data, it can be seen that the bionic fishtail developed in this paper approximates the performance of a real fishtail. The current research provides

a good basis for the development of a biomimetic robotic fish actuated by SMA wires.

To improve the performance of the biomimetic fishtail, future research should focus on the study of the accurate control of SMA wires, including a self-sensing controlling method based on resistance feedback and cooling techniques. We believe such research will help to make a higher oscillation frequency of the biomimetic fishtail and explore more possibilities.

APPENDIX ABBREVIATIONS

BCF	Body and/or Caudal Fin propulsion
IPMC	Ionic Polymer Metal Composites
MCU	Microcontroller Unit
MPF	Media and/or Paired Fin propulsion
PVC	Polyvinyl Chloride
SMA	Shape memory alloy
SME	Shape memory effect

REFERENCES

- W. Zou, W. Jing, G. Chen, Y. Lu, and H. Song, "A survey of big data analytics for smart forestry," *IEEE Access*, vol. 7, pp. 46621–46636, 2019.
- R. K. Katzschmann, A. D. Marchese, and D. Rus, "Hydraulic autonomous soft robotic fish for 3D swimming," in *Experimental Robotics*, vol. 109, 2016, pp. 405–420.
- R. K. Katzschmann, J. DelPreto, R. MacCurdy, and D. Rus, "Exploration of underwater life with an acoustically controlled soft robotic fish," *Sci. Robot.*, vol. 3, no. 16, p. eaar3449, 2018.
- F. E. Fish, "Limits of nature and advances of technology: What does biomimetics have to offer to aquatic robots?" *Appl. Bionics Biomechan.*, vol. 3, no. 1, pp. 49–60, 2006.
- R. W. Blake, "Fish functional design and swimming performance," *J. Fish Biol.*, vol. 65, no. 5, pp. 1193–1222, 2004.
- Y. S. Ryu, G.-H. Yang, J. Liu, and H. Hu, "A school of robotic fish for mariculture monitoring in the sea coast," *J. Bionics Eng.*, vol. 12, no. 1, pp. 37–46, Jan. 2015.
- J. Ayers, J. Witting, C. Wilbur, P. Zavracky, N. McGruer, and D. Massa, "Biomimetic robots for shallow water mine countermeasures," in *Proc. Auton. Vehicles Mine Countermeasures Symp.*, Monterey, CA, USA, 2000, pp. 1–16.
- S.-H. Song, M.-S. Kim, H. Rodrigue, J.-Y. Lee, J.-E. Shim, M.-C. Kim, W.-S. Chu, and S.-H. Ahn, "Turtle mimetic soft robot with two swimming gaits," *Bioinspiration Biomimetics*, vol. 11, no. 3, 2016, Art. no. 036010.
- J. Najem, S. A. Sarles, B. Akle, and D. J. Leo, "Biomimetic jellyfish-inspired underwater vehicle actuated by ionic polymer metal composite actuators," *Smart Mater. Struct.*, vol. 21, no. 9, 2012, Art. no. 094026.
- A. Villanueva, C. Smith, and S. Priya, "A biomimetic robotic jellyfish (Robojelly) actuated by shape memory alloy composite actuators," *Bioinspiration Biomimetics*, vol. 6, no. 3, 2011, Art. no. 036004.
- Y. Tadesse, A. Villanueva, C. Haines, D. Novitski, R. Baughman, and S. Priya, "Hydrogen-fuel-powered bell segments of biomimetic jellyfish," *Smart Mater. Struct.*, vol. 21, no. 4, 2012, Art. no. 045013.
- M. A. Kazemi-Lari, A. D. Dostine, J. Zhang, A. S. Wineman, and J. A. Shaw, "Robotic jellyfish actuated with a shape memory alloy spring," *Proc. SPIE*, vol. 10965, Mar. 2019, Art. no. 1096504, doi: 10.1117/12.2513456.
- M. Shibata and N. Sakagami, "Fabrication of a fish-like underwater robot with flexible plastic film body," *Adv. Robot.*, vol. 29, no. 1, pp. 103–113, 2015.
- W.-S. Chu, K.-T. Lee, S.-H. Song, M.-W. Han, J.-Y. Lee, H.-S. Kim, M.-S. Kim, Y.-J. Park, K.-J. Cho, and S.-H. Ahn, "Review of biomimetic underwater robots using smart actuators," *Int. J. Precis. Eng. Manuf.*, vol. 13, no. 7, pp. 1281–1292, 2012.
- M. Eftekhari, S. Rahmianian, and P. Moradi, "Analysis of bio-inspired kinematic patterns pectoral fin with shape memory alloy (SMA)," *Amer. J. Data Mining Knowl. Discovery*, vol. 2, no. 1, pp. 1–7, 2017.
- A. Suleman and C. Crawford, "Design and testing of a biomimetic tuna using shape memory alloy induced propulsion," *Comput. Struct.*, vol. 86, nos. 3–5, pp. 491–499, 2008.
- Z. Chen, S. Shatara, and X. Tan, "Modeling of biomimetic robotic fish propelled by an ionic polymer–metal composite caudal fin," *IEEE/ASME Trans. Mechatronics*, vol. 15, no. 3, pp. 448–459, Jun. 2010.
- Q. Shen, T. Wang, J. Liang, and L. Wen, "Hydrodynamic performance of a biomimetic robotic swimmer actuated by ionic polymer–metal composite," *Smart Mater. Struct.*, vol. 22, no. 7, 2013, Art. no. 075035.
- Q. S. Nguyen, S. Heo, H. C. Park, and D. Byun, "Performance evaluation of an improved fish robot actuated by piezoceramic actuators," *Smart Mater. Struct.*, vol. 19, no. 3, 2010, Art. no. 035030.
- A. Erturk and G. Delporte, "Underwater thrust and power generation using flexible piezoelectric composites: An experimental investigation toward self-powered swimmer-sensor platforms," *Smart Mater. Struct.*, vol. 20, no. 12, 2011, Art. no. 125013.
- S. T. McGovern, M. Abbot, R. Emery, G. Alici, V.-T. Truong, G. M. Spinks, and G. G. Wallace, "Evaluation of thrust force generated for a robotic fish propelled with polypyrrole actuators," *Polym. Int.*, vol. 59, no. 3, pp. 357–364, 2010.
- A. D. Marchese, C. D. Onal, and D. Rus, "Autonomous soft robotic fish capable of escape maneuvers using fluidic elastomer actuators," *Soft Robot.*, vol. 1, no. 1, pp. 75–87, 2014.
- M. Sfakiotakis, D. M. Lane, and J. B. C. Davies, "Review of fish swimming modes for aquatic locomotion," *IEEE J. Ocean. Eng.*, vol. 24, no. 2, pp. 237–252, Apr. 1999.
- S. Li and J. Li, "A robot fish of autonomous navigation with single caudal fin," in *Proc. 2nd Int. Conf. Robot. Automat. Eng. (ICRAE)*, Shanghai, China, Dec. 2017, pp. 276–279.
- H.-S. Kim, J.-Y. Lee, W.-S. Chu, and S.-H. Ahn, "Design and fabrication of soft morphing ray propulsor: Undulator and oscillator," *Soft Robot.*, vol. 4, no. 1, pp. 49–60, 2017.
- H. Rodrigue, W. Wang, M.-W. Han, T. J. Y. Kim, and S.-H. Ahn, "An overview of shape memory alloy-coupled actuators and robots," *Soft Robot.*, vol. 4, no. 1, pp. 3–15, 2017.
- C. Rossi, J. Colorado, W. Coral, and A. Barrientos, "Bending continuous structures with SMAs: A novel robotic fish design," *Bioinspiration Biomimetics*, vol. 6, no. 4, 2011, Art. no. 045005.
- Q. Yan, L. Wang, B. Liu, J. Yang, and S. Zhang, "A novel implementation of a flexible robotic fin actuated by shape memory alloy," *J. Bionic Eng.*, vol. 9, no. 2, pp. 156–165, 2012.
- W. Coral, C. Rossi, O. M. Curet, and D. Castro, "Design and assessment of a flexible fish robot actuated by shape memory alloys," *Bioinspiration Biomimetics*, vol. 13, no. 5, 2018, Art. no. 056009.
- P. Sheri and P. Rajagopal, "Shape memory alloy-based flexible manipulator for miniature submersible robots," *Proc. SPIE*, vol. 10968, Mar. 2019, Art. no. 109680Z.
- K. H. Low, "Current and future trends of biologically inspired underwater vehicles," in *Proc. IEEE Defense Sci. Res. Conf. Expo (DSR)*, Singapore, Aug. 2011, pp. 1–8.
- J. Liu and H. Hu, "Biological inspiration: From carangiform fish to multi-joint robotic fish," *J. Bionic Eng.*, vol. 7, no. 1, pp. 35–48, 2010.
- J. M. Anderson, K. Streitlien, D. S. Barrett, and M. S. Triantafyllou, "Oscillating foils of high propulsive efficiency," *J. Fluid Mech.*, vol. 360, pp. 41–72, Apr. 1998.
- C. S. Wardle and J. J. Videler, *Fish Swimming*. Cambridge, U.K.: Cambridge Univ. Press, 1980.
- Z. Wang, G. Hang, J. Li, Y. Wang, and K. Xiao, "A micro-robot fish with embedded SMA wire actuated flexible biomimetic fin," *Sens. Actuators A, Phys.*, vol. 2, no. 10, pp. 354–360, 2008.
- Z. Wang, G. Hang, Y. Wang, and J. Li, "Embedded SMA wire actuated biomimetic fin: A module for biomimetic underwater propulsion," *Smart Mater. Struct.*, vol. 17, no. 2, 2008, Art. no. 025039, doi: 10.1088/0964-1726/17/2/025039.
- C. Liang and C. A. Rogers, "One-dimensional thermomechanical constitutive relations for shape memory materials," *J. Intell. Mater. Syst. Struct.*, vol. 8, no. 4, pp. 285–302, 1990.

- [38] L. C. Brinson, "One-dimensional constitutive behavior of shape memory alloys: Thermomechanical derivation with non-constant material functions and redefined martensite internal variable," *J. Intell. Mater. Struct.*, vol. 4, no. 2, pp. 229–242, 1993.
- [39] G. V. Lauder and E. Drucker, "Forces, fishes, and fluids: Hydrodynamic mechanisms of aquatic locomotion," *News Physiol. Sci.*, vol. 17, no. 6, pp. 235–240, 2002.



JIAN LI (M'85) received the B.S. degree in mechanical engineering from Shandong University, Jinan, China, in 2005, and the M.S. and Ph.D. degrees in mechanical engineering from the Harbin Institute of Technology, Harbin, China, in 2007 and 2011, respectively.

From 2012 to 2016, he was a Lecturer with the College of Mechanical and Electrical Engineering, Northeast Forestry University, Harbin, where he has been an Associate Professor, since 2016. His

research interests include smart materials and robotics.

Dr. Li is a member of the Chinese Society of Forest and the Heilongjiang Mechanical Engineering Society. He is also a Review Expert of the journal *Engineering Applications of Computational Fluid Mechanics and Robot*.

JUNMIN HE, photograph and biography not available at the time of publication.



YANGWEI WANG (M'80) received the B.S. degree in mechanical engineering from the Nanjing University of Aeronautics and Astronautics, Nanjing, Jiangsu, China, in 2002, and the M.S. and Ph.D. degrees in mechanical engineering from the Harbin Institute of Technology, Harbin, China, in 2007 and 2011, respectively.

From 2011 to 2017, he was a Lecturer with the College of Mechanical and Electrical Engineering, Nanjing University of Aeronautics and Astronautics.

Since 2017, he has been an Associate Professor with the College of Mechanical and Electrical Engineering, Northeast Forestry University, Harbin. His research interests include smart materials and robotics.

Dr. Wang is a member of the International Society of Bionic Engineering and the Chinese Society of Aeronautics and Astronautics. He is also a Review Expert of the *IEEE Robotics and Automation Magazine* and the *Journal of Bionic Engineering*.

KAI YU, photograph and biography not available at the time of publication.



MARCIN WOŹNIAK received the Diploma degree in applied mathematics and computational intelligence, the master's degree from the Silesian University of Technology, in 2007, and the Ph.D. degree from the Czestochowa University of Technology, in 2012.

He is currently an Associate Professor with the Institute of Mathematics, Silesian University of Technology, Gliwice, Poland. In his scientific career, he visited the University of Würzburg, Germany, in 2007 (for part of the studies), the University of Lund, Sweden, in 2016 (as a guest of the ministerial program for young research professors), and the University of Catania, Italy, in 2015 and 2017 (as an Invited Professor for research projects and grants). His main scientific interests are neural networks with their applications together with various aspects of applied computational intelligence.

Dr. Woźniak is a Scientific Supervisor in editions of the Diamond Grant and The Best of the Best programs for highly gifted students from the Polish Ministry of Science and Higher Education. He has been an Organizer and the Session Chair in various international conferences and symposiums, such as the IEEE SSCI, the IEEE FedCSIS, APCASE, ICIST, ICAISC, and WorldCIST.



WEI WEI received the M.S. and Ph.D. degrees from Xi'an Jiaotong University, in 2005 and 2011, respectively.

He is currently an Associate Professor with the Xi'an University of Technology. His research interests include wireless networks and wireless sensor network applications, mobile computing, distributed computing, and pervasive computing.

• • •